JPEDAV (2014) 35:384–395
DOI: 10.1007/s11669-014-0291-0
1547-7037 ©ASM International

Crystal Structure of $W_{1-x}B_3$ and Phase Equilibria in the Boron-Rich Part of the Systems Mo-Rh-B and W-{Ru,Os,Rh,Ir,Ni,Pd,Pt}-B

I. Zeiringer, P. Rogl, A. Grytsiv, J. Polt, E. Bauer, and G. Giester

(Submitted December 19, 2013; in revised form February 5, 2014; published online March 13, 2014)

The crystal structure of $W_{1-x}B_3$ has been reinvestigated by x-ray single crystal diffraction and revealed isotypism with the $Mo_{1-x}B_3$ structure type (space group $P6_3/mmc$; a = 0.52012(1), c = 0.63315(3) nm; R_F = 0.040). As a characteristic feature of the structure, planar hexagonal metal layers (1/3 of atoms removed from ordered positions) sandwich planar boron honeycomb layers. One of the two W-sites shows a random defect of about 73%. Strong metal boron and boron-boron bonds are responsible for high mechanical stability. Although $W_{1-x}B_3$ at about 80 at.% B is the metal boride richest in boron, it contains no directly linked three-dimensional boron framework. The solubility of Rh, Ir, Ni, Pd and Pt in $W_{1-x}B_3$ as well as of Rh in $Mo_{1-x}B_3$ has been investigated in as cast state and after annealing. Furthermore, phase equilibria in the boron rich part of the corresponding isothermal sections W-TM-B (TM = Rh, Ir at 1100 °C, TM = Ni, Pd at 900 °C and TM = Pt at 800 °C) and Mo-Rh-B (at 1100 °C) have been established. A ternary compound only forms in the system W-Ir-B: τ_1-$W_{1-x}Ir_xB_2$ with ReB_2 structure type (space group $P6_3/mmc$; a = 0.2900, c = 0.7475 nm). The type of formation and crystal structure of diborides $W_{1-x}TM_xB_2$ (TM = Ru, Os, Ir) isotypic with ReB_2 were studied by x-ray powder diffraction and electron probe microanalysis in as cast state and after annealing at 1500 °C. Accordingly, $W_{0.5}Os_{0.5}B_2$ (a = 0.29127(1), c = 0.7562(1) nm) forms directly from the melt, whereas $W_{0.4}Ru_{0.6}B_2$ (a = 0.29027(1), c = 0.74673(2) nm) and $W_{0.6}Ir_{0.4}B_2$ (a = 0.29263(1), c = 0.75404(8) nm) are incongruently melting. Annealing at 1500 °C leads in case of the iridium compound to an almost single-phase product but the same procedure does not increase the amount of the ruthenium diboride.

Keywords crystal structure, isothermal section, ternary system, x-ray structure analyses

1. Introduction

Superhard materials (i.e. a material with a hardness surmounting 40 GPa[1-4]) are generally found in three different categories: (I) crystalline and disordered carbon modifications, (II) compounds formed by the light elements B, C, N, O, Si and (III) compounds of transition metals (TMs) with light elements B, C, N or O.[5,6] The main important parameters guiding high hardness have been identified as (i) the presence of directional covalent bonding and (ii) a high electron concentration (electrons per atomic volume) of the transition metal (TM).[6,7] Among borides particularly those richest in boron in the systems with W ("WB_4" at about 80 at.% B) and Re ("ReB_2" at about 66.7 at.% B) have triggered intensive research interest as potential superhard compounds. Although in many cases indentation hardness values beyond 40 GPa have been measured at miniaturized loads, load independent hardness, which essentially characterizes the true hardness of a material, never surpassed the superhardness criterion of 40 GPa. In the following we list a few of these examples referring to transition metal borides. "WB_4" was reported to possess a load independent Vickers hardness of 31.8 GPa (but 46.2 GPa at 0.5 N).[6] Load dependent hardness measurements and Re substitution studies by Mohammadi et al.[8] yield a load independent hardness of 28.1 GPa (but 43.3 GPa at 0.5 N) for WB_4 and an increase to 32.5 GPa (49.8 GPa (0.5 N)) with an addition of about 1 mol% Re. Polycrystalline ReB_2 exceeds an average load independent Vickers hardness of about 30 GPa (48 GPa (0.5 N))[9] or 26.6 GPa (39.3 GPa (0.5 N))[6] with rather different hardness values obtained due to the anisotropic crystal structure. From Vickers hardness measurements on various crystallographic planes of a single crystal, Levine et al.[10] determined the crystallographic (002) plane to be the hardest of ReB_2. The isotypic substitution of Re by W/Os, W/Ir and W/Ru has been studied first by Rogl and coworkers.[11,12] Vickers hardness measurements on $W_{0.5}Os_{0.5}B_2$ revealed a load independent hardness of 26.6 GPa (40.4 GPa

Dedicated in memoriam Prof. Dr. Fred Hayes.

I. Zeiringer, P. Rogl, A. Grytsiv, and **J. Polt**, Institute of Physical Chemistry, University of Vienna, Waehringerstr. 42, 1090 Wien, Austria; **E. Bauer**, Institute of Solid State Physics, Vienna University of Technology, Wiedner Hauptstr. 8-10, 1040 Wien, Austria; and **G. Giester**, Institute of Mineralogy and Crystallography, University of Vienna, Althanstr. 14, 1090 Wien, Austria. Contact e-mail: isolde.zeiringer@ univie.ac.at and peter.franz.rogl@univie.ac.at.

(0.5 N))[6] and single crystal studies confirmed the ReB_2 structure type with a random occupancy of the TM site.[6] As the hardness of a material above the asymptotic leveling is not meaningful,[13,14] all the aforementioned compounds cannot be considered as superhard materials but nevertheless are among the hardest metal borides.

Despite several structure models have been proposed in the past for the boron richest W-boride,[15-19] $W_{1-x}B_3$ ("WB_4"), the structure type of isotypic $Mo_{1-x}B_3$[19] has been widely accepted. However, more recent theoretical calculations of band structure and physical properties (density functional theory calculations DFT) of this compound have inferred some confusion on the true crystal structure of "WB_4".[20-26] Whereas the first studies by Chretien and Helgorsky[15] reported a tetragonal unit cell for "WB_4" (a = 0.634 nm, c = 0.450 nm), Rudy et al.[16] claimed a hexagonal cell (a = 0.3004 nm, c = 0.3174 nm) but proposed "WB_{12}" as a more appropriate composition. A first structure model was derived by Romans and Krug[17] from x-ray powder data backed by single crystal Laue and precession photographs indexed on a hexagonal lattice (a = 0.5200 nm, c = 0.6340 nm). The proposed structure of stoichiometric WB_4 was derived from the AlB_2 structure, by replacing one third of the metal atoms by pairs of boron atoms (dumbbells) linking the two-dimensional planar boron layers into a three-dimensional covalently bonded boron framework.[17] The boron dumbbells are located just in the voids (two per unit cell) created by the metal atom missing in the planar hexagonal closed packed metal atom layers at z = 1/4, 3/4. Independently Nowotny et al.[18] proposed a similar structure on the basis of x-ray powder and rotating crystal data (a = 0.5206 nm, c = 0.6335 nm), where $[B_6]$-octahedra replace one third of the metal atoms in the hexagonal metal layer creating a three-dimensional boron-skeleton at a composition of $W_{2-x}B_9$ (x = 1/6 ≡ $W_{17}B_{83}$ in at.%). Nowotny et al.[18] also evaluated the relation among the different sets of unit cell dimensions (see Fig. 1).

From the x-ray powder spectra reported there is no doubt that the phases "WB_4" and "$W_{2-x}B_9$" of the various aforementioned research groups[15-18] are all identical and secondly are isotypic with the homologous phases observed in the Mo-B system: "MoB_4" and "$Mo_{2-x}B_9$"[15-19] Nowotny et al.[18] furthermore reported on a considerable solubility of Rh, Ni, Pd and Pt in $W_{2-x}B_9$ and particularly the PhD work of Haschke[27] indicated the existence of ternary compounds $(Mo, Rh)_{2-x}B_9$ and $(W, M)_{2-x}B_9$ (M = Rh, Ni, Pd, Pt) at 900 °C.

Lundström and Rosenberg[19] analyzed in detail the x-ray powder pattern of the crystal structure of $Mo_{1-x}B_3$ (x~0.2; $P6_3/mmc$, a = 0.52026 nm, c = 6.3489 nm, B-rich) from which they derived defect close-packed metal layers sandwiched by planar boron honeycomb layers stacked along the c-direction.[19] There are no direct B-B contacts between B-layers. The boron honeycomb layers in z = 0 are planar[17,19] or slightly puckered;[18] a planar boron honeycomb layer also exists in the structures at z = 0.5[17,19]. Lundström and Rosenberg[19] confirmed isotypism with the homologous $W_{1-x}B_3$.

The theoretical DFT studies on the structural assignment and stability of WB_4 or MoB_4 (WB_3 or MoB_3)[20-26]

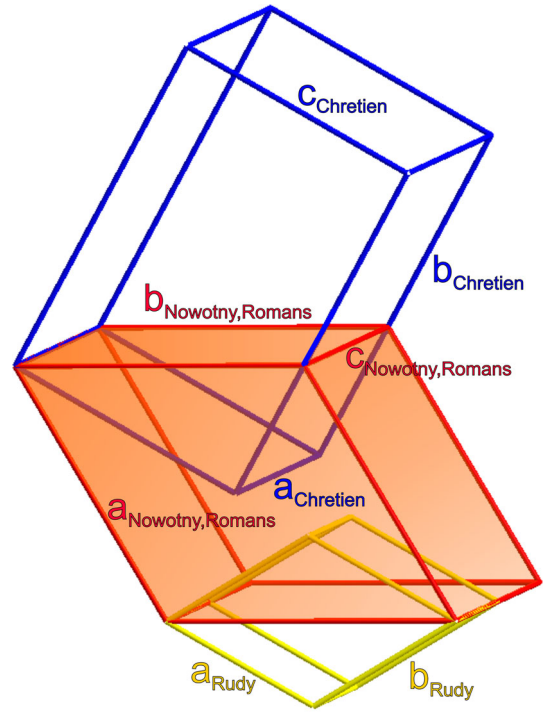

$$a_{Now,Rom} \equiv a_{Rudy}\sqrt{3} \equiv c_{Chretien}\frac{2}{\sqrt{3}}$$

$$c_{Nowotny,Romans} \equiv 2c_{Rudy} \equiv a_{Chretien}$$

Fig. 1 Relation of the different unit cell propositions for "WB_4" from Nowotny et al.,[18] Romans and Krug,[17] Rudy et al.[16] and Chretien et al.[15]

claimed that WB_3 (MoB_3) with a two-dimensional boron net is thermodynamically more stable than WB_4 (MoB_4) with a three-dimensional boron skeleton.[20-26] Zhang et al.[24] reopened the question on the correct crystal structure of WB_4 or WB_3, as the calculated indentation hardness of WB_4 is lower than that of ReB_2 in contrast to the experimental result and the calculated normalized c/a ratio of WB_3 exhibits a negative pressure dependence, inconsistent with the observed trend. Li et al.[25] in their latest study presented new thermodynamically stable structures for WB_3 ($R\,\bar{3}m$-"6u") and WB_4 ($P6_3/mmc$-"2u"). However, the DFT stability calculations so far never considered nonstoichiometric $W_{1-x}B_3$ with defects in metal atom sites.

As most transition metal diborides exhibit superconductivity, Simonson et al.[28] tested various transition metal-doped alloys $Mo_{1-x}M_xB_4$ (M = Ti, Zr, Hf, V, Nb, Ta, Re) and the corresponding $W_{1-x}M_xB_4$ alloys. Indeed Ti and Nb doped $Mo_{1-x}M_xB_4$ alloys were claimed to reveal superconductivity below critical temperatures around 6.5 K (Ti) and 7.5 K (Nb), whereas no superconductivity has been detected in all the tungsten-based alloys.

In view of all these inconsistencies among experimental and DFT structural information, the tasks of the present work are (i) to elucidate the crystal structure of $W_{1-x}B_3$ by single crystal x-ray diffraction, (ii) to define the solubility of Rh, Ir, Ni, Pd and Pt in $W_{1-x}B_3$ as well as of Rh in $Mo_{1-x}B_3$

(iii) to establish the phase equilibria in the boron rich part of the isothermal sections W-TM-B at 1100 °C (TM = Rh, Ir), at 900 °C (TM = Ni, Pd) and at 800 °C for TM = Pt and of Mo-Rh-B at 1100 °C and (iv) to study formation and crystal structure of ReB_2 isotypic compounds in the ternary systems W-TM-B (TM = Ru, Os, Ir) and V-Ir-B in as cast state and at 1500 °C.

2. Experimantal Details

Stoichiometric quantities of powders of vanadium, tungsten, molybdenum, iridium, rhodium (purity 99.99%), nickel and crystalline boron (purity 98-99%) were carefully mixed, cold-compacted to pellets and melted in an arc furnace under argon at least three times to ensure homogeneity. For the samples with Pd or Pt, metal ingots were used. The arc-melted buttons were cut into pieces, wherefrom one piece was wrapped in tantalum foil and vacuum-sealed in a quartz tube for annealing at 800, 900 or 1100 °C. The samples $(W_{1-x}TM_x)B_2$ (TM = Ru, Os, Ir) and $V_{17}Ir_{16}B_{67}$ were annealed at 1500 °C for 48 h on a BN-substrate in a high vacuum furnace of 3×10^{-4} Pa with a W-sheet metal heater. All samples were characterized in as cast state and after annealing by scanning electron microscopy (SEM), electron probe microanalysis (EPMA) on a Zeiss Supra 55 VP operated at 20 kV and 60 μA using EDX and WDX detection for the quantitative analysis) and x-ray powder diffraction (XPD, Guinier-Huber image plate recording system, Cu-Kα_1 radiation). X-ray single crystal diffraction data (XSCD) were collected on a four-circle Nonius Kappa diffractometer with C-monochromated Mo-Kα radiation. The DSC measurements have been carried out on the annealed samples in a Netzsch 404 Pegasus DSC equipment under a stream of 6N argon and heating rates of 5 K/min. The equipment was calibrated in the temperature range from 300 to 1400 °C against pure standard metals supplied by Netzsch to be within ±1 °C.

Further details of the characterization techniques can be found in our previous paper.[29]

3. Results and Discussion

3.1 The Crystal Structure of $W_{1-x}B_3$

As described in the introduction the compound $W_{1-x}B_3$ (or WB_4) is already known since the early 1960s, its correct crystal structure, however, seems to be still under debate, because the established isotypism of $W_{1-x}B_3$[15-18] with the structure type of $Mo_{1-x}B_3$[19] has been ignored in more recent studies.[20-26] As boron is difficult to detect by x-rays beside such a heavy metal element, several propositions have been made concerning the arrangement of the boron atoms in the crystal structure. Table 1 presents a listing of the crystallographic parameters for the three different structural models reported in the literature, which have been established for WB_4,[17] $W_{2-x}B_9$[18] and for $Mo_{1-x}B_3$.[19] At the bottom of Table 1 one can compare these structure models in three-dimensional view. All structure models agree on planar hexagonal metal layers from which 1/3 of the atoms is removed. However, a (additional) significant metal atom defect in the crystallographic site (0, 0, 0.25) was only described for $W_{2-x}B_9$ ($\equiv W_{1.83}B_9$)[18] and for $Mo_{1-x}B_3$ ($\equiv Mo_{0.80}B_3$).[19]

To reinvestigate the crystal structure, a single crystal has been selected from the crushed arc-melted sample with nominal composition WB_9. The observed extinctions are consistent with the space groups *$P6_3mc$, $P\bar{6}2c$ or $P6_3/mmc$.* The crystal structure has been solved employing direct methods (using SHELX[30] in the program OSCAIL[31]) in the hexagonal space group with highest symmetry *$P6_3/mmc$* (Nr.194; a = 0.52012(1), c = 0.63315(3) nm). Although direct methods prompt the crystallographic sites 2c (1/3, 2/3,1/4) and 2b (0,0,1/4) for the heavy scatterers i.e. the W atoms, the Fourier series undoubtedly reveals a reduced occupancy for the latter site (2b) of only about 72% (see Table 2). The metal defects in 2b appear randomly as there is no indication for a long-range metal/vacancy order. Boron atoms are located from the difference Fourier and occupy only the Wyckoff site 12i (x,0,0) leading to the final composition $W_{0.86}B_3$ ($\equiv W_{22}B_{78}$ in at.%). Table 2 comprises the results of the single crystal refinement, which converged to a final R-factor R_F = 0.040 employing anisotropic atom displacement parameters for the W-sites but isotropic temperature factors for the boron atom. The largest residual electron density and the deepest hole (6.62; −6.23 e/Å^3) are close (~0.4 Å) to the tungsten atom in the 2c site and merely reflect the Fourier ripples to the large W-peak. It should be emphasized that the residual electron density reveals neither hints for B-B dumbbells nor for B_6 octahedra as proposed earlier in Ref [17,19]. Wyckoff sequence and atom positions in $W_{0.86}B_3$ confirm isotypism with the structure model presented by Lundström and Rosenberg for $Mo_{1-x}B_3$. A three-dimensional view on the crystal structure of $W_{1-x}B_3$ is shown in Fig. 2, which also presents the coordination polyhedra for all atom sites. The structure solution obtained from the single crystal data fits well with the XPD data as can be seen from the Rietveld refinement (using the FULLPROF program[32]) in the right part of Fig. 2. The interatomic bonding distances in Table 2 merely reflect strong metal-boron bonding in the coordination figures as $d_{W\text{-}B}$ = 0.235 nm is always smaller than the sum of the W-metal (R_W = 0.139 nm) and covalent B-radius (R_B = 0.088 nm).[33] The in-plane boron boron contacts $d_{B\text{-}B}$ = 0.173 nm are fully consistent with the covalent radius sum, but W-W contacts $d_{W\text{-}W}$ = 0.300 nm are slightly larger than the sum of their metal atom radii. As seen from Fig. 1 the metal coordination around the B-atom is a truncated triangular tungsten prism of which only 4 next nearest neighbours remain in form of a rather distorted tetrahedron. The strong metal-boron and boron-boron bonds in the structure are responsible for the high mechanical stability i.e. the high hardness and the ultra-incompressibility discussed in the literature[20-26] similar to the transition metal diborides.[34] It should be mentioned that the two identical next nearest neighbour coordination figures around the two W-sites do not contain any hint for the defect in the W2 site—this may be explained in future DFT calculations.

Table 1 Comparison of different structural models in standardized settings for WB_4 or $W_{2-x}B_9$ and the isotypic compound $Mo_{1-x}B_3$; only the B-B and metal-metal bonds are drawn in the unit cells

	Romans and Krug[17]; stoichiometric WB_4	Nowotny et al. [18]; $W_{2-x}B_9$ (x~1/6 ≡ $W_{0.61}B_3$)	Lundström and Rosenberg [19]; $Mo_{1-x}B_3$ (x~0.2 ≡ $Mo_{0.80}B_3$)
Space group	$P6_3/mmc$	$P\bar{3}$	$P6_3/mmc$
Lattice parameter, nm	a = 0.5200	a = 0.5026	a = 0.52026(2)
	c = 0.6340	c = 0.6335	c = 0.63489(3)
			B-rich
$R_I = \Sigma\|I_0-I_c\|/\Sigma I_0$	...	...	0.088
Atomic parameter			
M1/Wycoff Pos.; Occ	W1 in 2c (1/3,2/3,1/4); 1	W1 in 2d (1/3,2/3,0.250); 1	Mo1 in 2c (1/3,2/3,1/4); 1
M2/Wycoff Pos.; Occ	W2 in 2b (0,0,1/4); 1	W2 in 2c (0,0,0.250); ~0.83	Mo2 in 2b (0,0,1/4); 0.60(4)
B1/Wycoff Pos.; Occ	12i (0.333,0,0); 1	6g (0.0,0.333,0.023); 1	12i (0.333,0,0); 1
B2/Wycoff Pos.; Occ	4f (1/3,2/3,0.615); 1 (form a dumbbel)	6g (0.472, 0.331, 0.202); 1	...
B3/Wycoff Pos.; Occ	...	6g (0.475, 0.141, 0.427);1	...
Unit cell	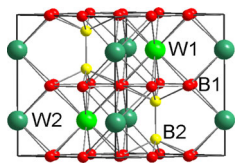	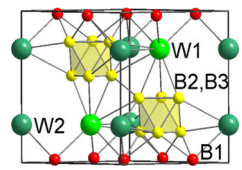	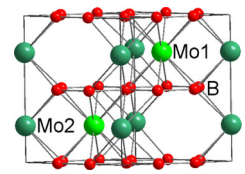

3.2 Isothermal Sections of the Boron Rich Part of the Ternary Systems W-TM-B (TM = Rh, Ir, Ni, Pd, Pt) and Mo-Rh-B

The isothermal sections {Mo,W}-Rh-B at 1100 °C, {Mo,W}-Ni-B at 900 °C, {Mo,W}-Pd-B at 950 °C, and Mo-Pt-B at 900 and 800 °C have been investigated by Haschke,[18,27] whilst phase relations in the ternary system W-Ir-B at 1200 °C were published by Rogl et al.[35] Haschke[27] reported in all the aforementioned tungsten-based ternary systems and in the Mo-Rh-B system at the respective temperatures a ternary phase labeled as $\{W(Mo)_{1-x}TM_x\}_2B_9$ (x~0.33 to 0.5) with the structure type of "$W_{2-x}B_9$" (≡ $Mo_{1-x}B_3$—type; see Fig. 3). Interestingly, the isothermal sections at these low temperatures neither contained the binary phase "$W_{2-x}B_9$" nor isotypic "$Mo_{2-x}B_9$", thus reporting the compounds $\{W(Mo)_{1-x}TM_x\}_2B_9$ as truly ternary phases. As thermal instability at lower temperatures was never reported for the binary borides richest in W or Mo (both at about 80 at.% B; for details see also Ref [36,37]), we decided to reinvestigate the boron rich part of these isotherms. Additionally, we studied the B-rich isothermal sections W-Ir-B and W-Pt-B at 1100 and 800 °C, respectively. We also investigated the possible solid solutions starting from binary $(W,Mo)_{1-x}B_3$ in as cast state and after annealing at 1100, 900 or 800 °C by XPD using Ge as a standard for the lattice parameter determination and EPMA. Crystallographic details of all appearing phases in the investigated regions are presented in Table 3. Results are summarized in Table 4 together with the lattice parameters reported in the literature. As various formulae have been reported in the literature, we refer to the formula $W_{1-x}B_3$ or $W_{1-x}TM_xB_3$ for an easier comparison in the column 'accepted composition' in Table 4. The 'accepted composition' for our alloys results from Rietveld refinement. We also investigated the solubility of Rh in $Mo_{1-x}B_3$ in as cast state and after annealing at 1100 °C. As a very accurate quantitative boron measurement is not possible by EPMA using EDX detection (see Table 4), we mainly focused in the samples with transition metals, on measuring the metal ratios. Information on the binary phase diagrams and phases for Mo-B, Rh-B, Ni-B and Pt-B is taken from Massalski,[38] for W-B from Duschanek and Rogl[36] and for Ir-B and Pd-B from Rogl.[39] Particularly the binary solid solubilities of the various transition metals in ß-rhombohedral boron in the temperature region from 900 to 1500 °C were taken from Crespo et al.[40] as less than 0.25 at.% for Mo and W (see also Rudy et al.[37]), and less than 0.1 at.% for Ru, Os, Rh, Ir. For vanadium (~1.5 at.% V at 1500 °C) and nickel (~2 at.% Ni at 900 °C) we follow the investigations of Garbouskas et al.[41] and Smid et al.,[42] respectively. For all systems investigated, except for the W-Ir-B system, a three-phase equilibrium exists between ßB, $W_{1-x}B_3$ or $Mo_{1-x}B_3$ and the transition metal boride richest in boron (RhB, NiB, Pd_2B, $PtB_{0,67}$, see Fig. 4). The peritectic formation of $W_{1-x}B_3$ around grains of WB_2 (labeled earlier as W_2B_{5-x}-type) is documented in all tungsten-based alloys (see microstructures in Fig. 4). The last liquid crystallizes in form of a transition metal rich boride or eutectic. The same can be derived from the microstructure of the Mo-Rh-B alloy. In the boron rich part of the isothermal section of the W-Ir-B system, a three-phase equilibrium exists between B, WB_2 and τ_1-$W_{1-x}Ir_xB_2$ (ReB_2-type) and another between B, Ir_4B_5 and τ_1 (see Fig. 4c). The invariant reaction temperatures were measured for all systems with DSC and are summarized in Table 5 together with the results from EPMA measurements and x-ray phase analysis. The DSC data on ternary reaction

Table 2 X-ray single crystal data for $W_{1-x}B_3$ at RT, standardized with program *Structure Tidy* (MoK-radiation; 2°≤2Θ≤70°; ω-scans, scan width 2°; 150 s/frame); Anisotropic displacement parameters in, (10^{-2}nm^2)

Parameter/compound			
Space group			$P6_3/mmc$
Formula from refinement			$W_{0.86}B_3$ (≡ $W_{22.3}B_{77.8}$ at.%)
a, c, nm			0.52012(1), 0.63315(3)
μ_{abs}, mm^{-1}			38.6
V, nm^3			0.1483
ρ_x, g cm^{-3}			8.55
Reflections in refinement			$152 \geq 4\sigma(F_o)$ of 159
Number of variables			7
$R_F = \Sigma\|F_0 - F_c\|/\Sigma F_0$			0.040
R_{Int}			0.040
wR2			0.119
GOF			1.207
Extinction (Zachariasen)			0.019(5)
Residual density e$^-$/Å^3; max; min			6.17; −6.28
Atom parameters			
W1 in 2c (1/3, 2/3, 1/4); occ			1
$U_{11} = U_{22} = U_{33}$			0.0018(6)
W2 in 2b (0,0,1/4); occ			0.725(7)
$U_{11} = U_{22} = U_{33}$			0.0019(5)
B1 in 12i (*x*, 0, 0); occ.			1
x			0.3341(8)
U_{iso}			0.0026(3)
Interatomic distances, nm: standard deviation <0.0001			
W1-	12B2	0.2346	
W2-	12B2	0.2351	
B1-	1B1	0.1725	
	−2B1	0.1738	
	−2W1	0.2346	
	−2B2	0.2346	
	−2W2	0.2350	

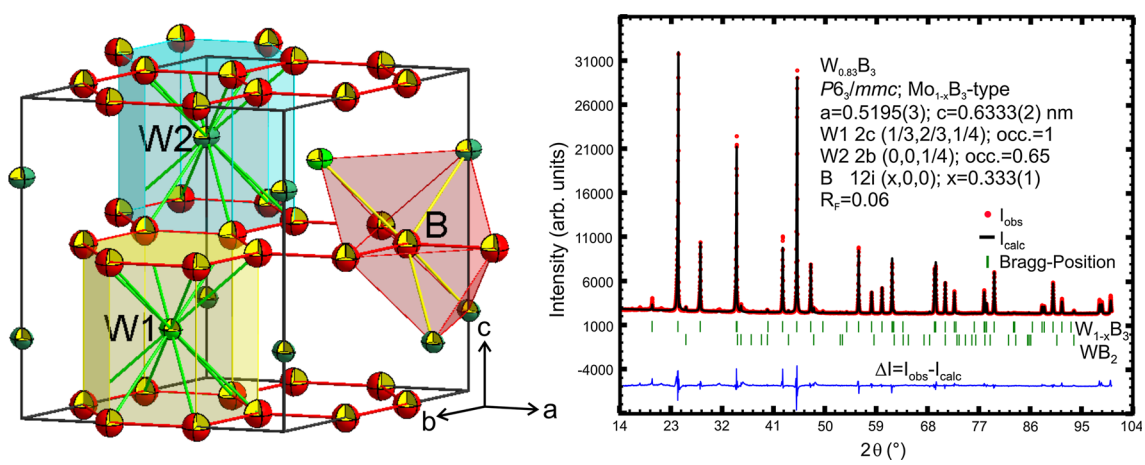

Fig. 2 Unit cell of $W_{1-x}B_3$ including coordination polyhedra for all atoms and Rietveld refinement of the x-ray powder pattern for $W_{0.83}B_3$

isotherms in Table 5 demonstrate that on heating liquification temperatures in the ternary systems investigated are all close to or slightly below the binary boron-rich TM-B eutectic temperatures. Above these temperatures "burning" of alloys may appear even close to the high melting Mo-B and W-B binaries.

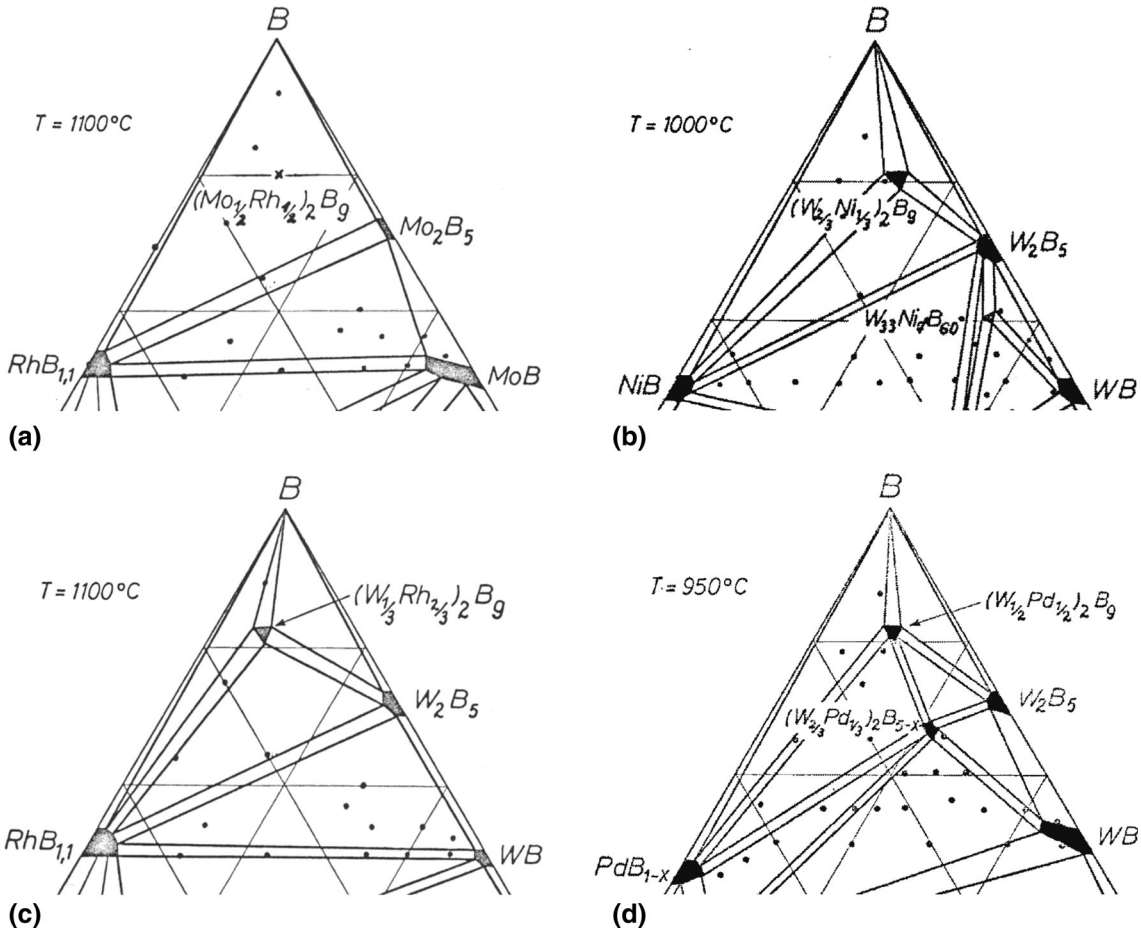

Fig. 3 Boron rich part of the isothermal sections of the ternary systems (a) Mo-Rh-B and (b) W-Ni-B at 1000 °C, (c) W-Rh-B at 1100 °C and (d) W-Pd-B at 950 °C; all as published by Haschke[27]

As a result of our investigations, the phase equilibria in the boron-rich parts of the systems {Mo,W}-Rh-B, {Mo,W}-{Ni,Pd,Pt}-B and W-Ir-B, all reveal the existence of binary borides with the $Mo_{1-x}B_3$-type (at about 80 at.% B) without any extension (solid solubilities) into the corresponding ternaries. Accordingly there is practically no difference between the lattice parameters (within the error bars) of the binary $Mo_{1-x}B_3$-type phases and those measured from ternary alloys (compare data in Tables 3 and 4). This argument also holds for a comparison of lattice parameters of the phases "$\{W(Mo)_{1-x}TM_x\}_2B_9$" reported by Haschke[18,27] with the binary $Mo_{1-x}B_3$-type borides. Ternary compounds neither appeared in as cast condition nor in annealed alloys. The reason for the severe discrepancy between (i) the existence of ternary compounds $\{W(Mo)_{1-x}TM_x\}_2B_9$ (x~0.33 to 0.5) as reported by Haschke[27] and (ii) the absence of ternary compounds but observation of isotypic phases in the binary with the structure type of "W_2B_9" (≡ $Mo_{1-x}B_3$-type), may be found (a) in the slow reaction kinetics of the binary peritectically formed borides $\{Mo,W\}_{1-x}B_3$ as well as (b) in the significantly enhanced reaction kinetics concomitant with the severely lowered melting and liquidus temperatures (see DSC data in Table 5) in the ternary systems investigated.

3.3 The Tungsten-Based Ternary Transition Metal Diborides $W_{1-x}TM_xB_2$ (TM = Ru, Os, Ir)

Isotypic diborides with the structure type of ReB_2 (space group $P6_3/mmc$; a = 0.2900, c = 0.7475 nm[43]) can be achieved by combination of metal elements from the 6th (Mo,W) and 8th (Ru,Os) group of the periodic table as they form a pseudo element from the 7th group. The electronegativity is approximately the same as for rhenium, if the metal ratio 6th/8th is ~1/2.[11,12] More general, all isotypic compounds keep an electron/atom ratio between 4.3 and 4.4[44] f. e. $V_{0.4}Os_{0.6}B_2$,[45] $W_{0.5}Ir_{0.4}B_2$[11,35] and $Mo_xIr_{1-x}B_2$ (x = 0.3, 0.6).[12,40] In this work, we investigated the type of formation and crystal structure of compounds with nominal composition $W_{13}Ru_{18}B_{69}$, $W_{15}Os_{16}B_{69}$, $W_{18}Ir_{13}B_{69}$ and $V_{17}Ir_{16}B_{67}$ in as cast state and after annealing at 1500 °C for 3 days. The compounds $W_{0.4}Ru_{0.6}B_2$ and $W_{0.6}Ir_{0.4}B_2$ (composition determined with EPMA, see Table 6) form incongruently (see Fig. 5a and c) whereas $W_{0.5}Os_{0.5}B_2$ forms directly from the melt (Fig. 5b). $W_{0.4}Ru_{0.6}B_2$ forms in a peritectic reaction around large primary grains of WB_2 (W_2B_{5-x}-type; Fig. 4a). However, annealing at 1500 °C does not change much the microstructure or composition of the appearing phases in the W-Ru-B system and therefore

Table 3 Crystallographic data on the solid phases of the boron rich part of the ternary systems W-TM-B (TM = Rh, Ir, Ni, Pd, Pt) and Mo-Rh-B

	Space group	Structure type	Lattice parameter, nm			Ref.
			a	*b*	*c*	
(B)	$R\bar{3}m$	βB	1.09382(5)	···	2.38356(18)	[38]
WB_2	$P6_3/mmc$	WB_2	0.29831(1)	···	1.38790(3)	[46]
RT-MoB_2	$R\bar{3}m$	MoB_2	0.30116(2)	···	2.0937(2)	[50]
HT-MoB_2	$P6/mmm$	AlB_2	0.30049(3)	···	0.31726(4)	[50]
$W_{1-x}B_3$	$P6_3/mmc$	$Mo_{1-x}B_3$	0.5207	···	0.6303	[18]
$Mo_{1-x}B_3$	$P6_3/mmc$	$Mo_{1-x}B_3$	0.52026(2)	···	0.63489(3)	[19]
RhB	$P6_3/mmc$	NiAs	0.3309	···	0.4224	[19]
Ir_4B_5	$C2/m$	Ir_4B_5	1.05300(9)	0.29038(3) β = 91.119(9)°	0.61013(5)	[19]
NiB	$Cmcm$	TlI	0.2929	0.7392	0.2961	[19]
Pd_2B	$Pnnm$	$CaCl_2$	0.46918(4)	0.51271(4)	0.31096(3)	[19]
$PtB_{0.67}$	$Cmcm$	$PtB_{0.67}$	0.3371(1)	0.5817(2)	0.4045(1)	[19]
$W_{0.52}Ir_{0.38}B_2$	$P6_3/mmc$	ReB_2	0.2926	···	0.7559	[12]
$W_{0.3}Ru_{0.7}B_2$	$P6_3/mmc$	ReB_2	0.2906	···	0.7452	[12]
$W_{0.3}Os_{0.7}B_2$	$P6_3/mmc$	ReB_2	0.2911	···	0.7497	[11]
$W_{0.5}Os_{0.5}B_2$	$P6_3/mmc$	ReB_2	0.29120(2)	···	0.75681(7)	[6]
RuB_2	$Pmmn$	RuB_2	0.46443(3)	0.28668(8)	0.40449(4)	[47]
OsB_2	$Pmmn$	RuB_2	0.4684	0.2872	0.4076	[48]
VB_2	$P6/mmm$	AlB_2	0.2998(2)	···	0.3057(2)	[49]

Table 4 Results from EPMA and XPD including literature data for $W_{1-x}B_3$, $W_{1-x}TM_xB_3$ and $Mo_{1-x}B_3$

Nominal composition	EPMA, at.%			Accepted composition(a)	Lattice parameter, nm		Heat treatment	Ref.
	W	TM	B		*a*	*c*		
WB_9	17.2	···	82.8	$W_{0.81}B_3$	0.51953(3)	0.6333(2)	As cast	This work
				$W_{0.86}B_3$	0.52012(1)	0.63315(3)SC		
WB_4	···	···	···	$W_{0.75}B_3$	0.5200	0.6340	As cast	[17]
$W_{1.83}B_9$	···	···	···	$W_{0.61}B_3$	0.5207	0.6303	1400 °C	[18]
WB_4	···	···	···	$W_{0.75}B_3$	0.5195(2)	0.6332(1)	1300 °C	[6]
$W_{0.5}Rh_2B_{7.5}$	16.4	···	83.6	$W_{0.8}B_3$	0.51981(5)	0.6331(1)	As cast	This work
	17.3	0.8	81.9	$W_{0.82}B_3$	0.52006(8)	0.6342(2)	1100 °C	
$(W_{1/3}Rh_{2/3})_2B_9$	···	···	···	$W_{0.22}Rh_{0.44}B_3$	0.520	0.627	1100 °C	[18,27]
$W_{0.8}Ir_2B_{7.2}$	26.4	···	73.6	$W_{0.8}B_3$	0.52001(3)	0.63249(7)	As cast	This work
$W_1Ni_{0.5}B_{8.5}$	23.0	0.8	76.2	$W_{0.8}B_3$	0.51990(5)	0.6334(2)	As cast	This work
	25.1	0.3	74.6	$W_{0.83}B_3$	0.51979(5)	0.63366(7)	900 °C	
$(W_{2/3}Ni_{1/3})_2B_9$	···	···	···	$W_{0.44}Ni_{0.22}B_3$	0.520	0.630	1000 °C	[18,27]
$W_{0.6}Pd_{1.4}B_8$	19.2	···	80.8	$W_{0.83}B_3$	0.51977(5)	0.6334(1)	As cast	This work
	21.8	0.1	78.1	$W_{0.85}B_3$	0.51962(6)	0.6331(1)	900 °C	
$(W_{1/2}Pd_{1/2})_2B_9$	···	···	···	$W_{0.33}Ni_{0.33}B_3$	0.520	0.631	950 °C	[18,27]
$W_{0.6}Pt_{1.4}B_8$	23.8	···	76.2	$W_{0.83}B_3$	0.51980(3)	0.63302(7)	As cast	This work
	24.6	···	75.4	$W_{0.83}B_3$	0.52006(2)	0.6333(2)	900 °C	
$(W_{2/3}Pt_{1/3})_2B_9$	···	···	···	$W_{0.44}Pt_{0.22}B_3$	0.520	0.631	1050 °C	[18,27]
$Mo_{1-x}B_3$	···	···	···	$Mo_{0.8}B_3$	0.52026(2)	0.63489(3)	1800 °C	[19]
$Mo_{1-x}B_3$	···	···	···	$Mo_{0.91}B_3$	0.52646(6)	0.6121(1)	1400 °C	[50]
$Mo_{0.8}Rh_2B_{7.2}$	18.0	0.1	81.9	$Mo_{0.82}B_3$	0.5209(2)	0.6348(3)	As cast	This work
	19.6	0.6	79.8	$Mo_{0.8}B_3$	0.51902(5)	0.6334(3)	1100 °C	

SC from single crystal
(a)From Rietveld refinement

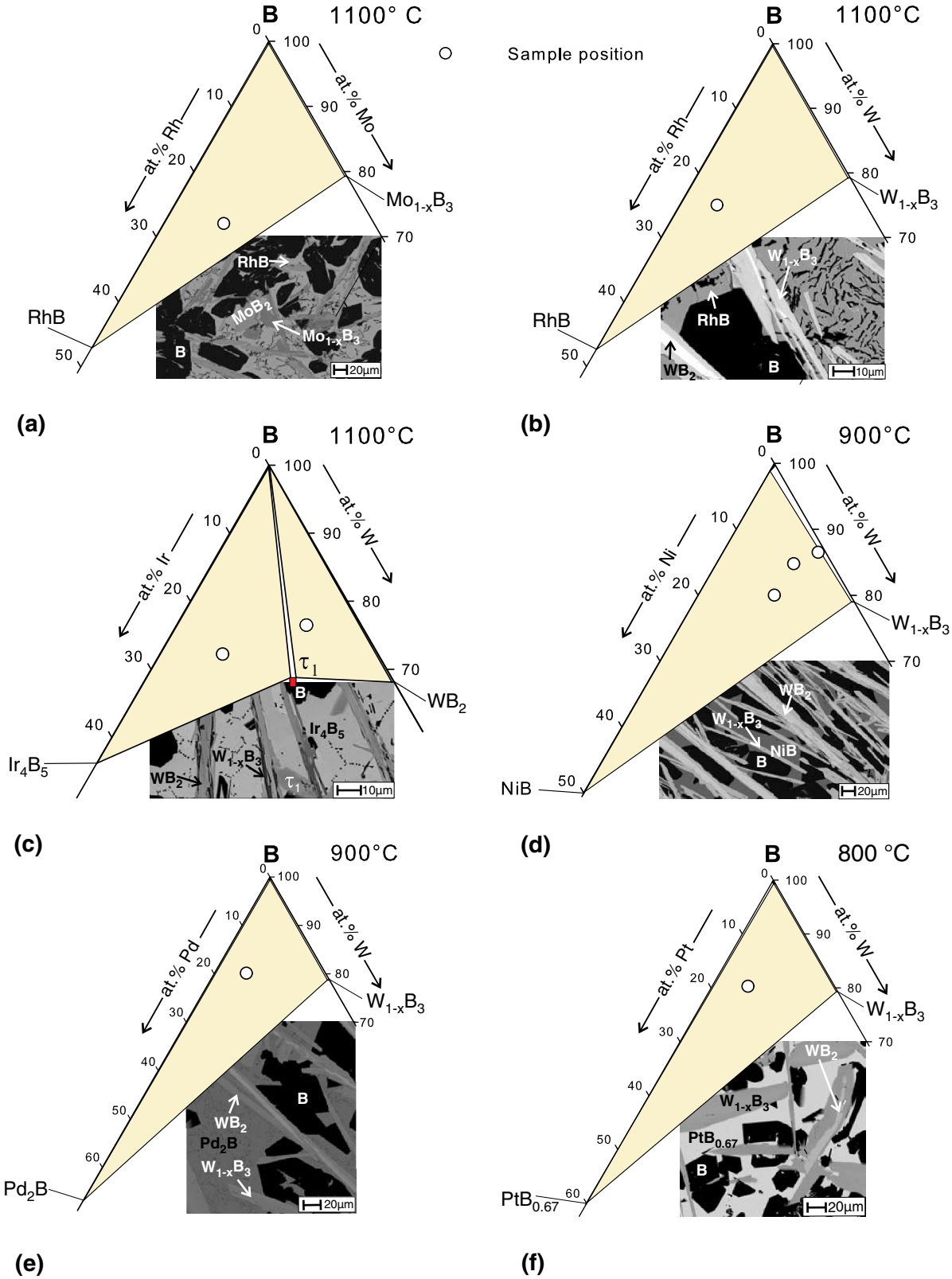

Fig. 4 Partial isothermal sections of the ternary systems (a) Mo-Rh-B and (b) W-Rh-B and (c) W-Ir-B at 1100 °C and of the ternary systems (d) W-Ni-B, (e) W-Pd-B at 900 °C and of (f) W-Pt-B at 800 °C. The shown microstructures are from the alloys in as cast state

Table 5 Results from EPMA measurements and x-ray phase analysis including invariant reaction temperatures from DTA measurements

Sample	Phases	Structure type	Composition EPMA, at.%			DTA °C	Lattice parameter, nm		
			Mo, W	TM	B		*a*	*b*	*c*
$Mo_{0.8}Rh_2B_{7.2}$	B	B	0.2	0.4	99.4	1115	···	···	···
1100	$Mo_{1-x}B_3$	$Mo_{1-x}B_3$	19.6	0.6	79.8		0.51902(5)	···	0.6334(3)
	RhB	NiAs	0.0	43.9	56.1		0.3313(2)	···	0.4218(2)
$W_{0.5}Rh_2B_{7.5}$	B	B	0.2	0.1	99.7	1115	···	···	···
1100	$W_{1-x}B_3$	$Mo_{1-x}B_3$	17.3	0.8	81.9		0.52006(8)	···	0.6342(2)
	RhB	NiAs	0.0	43.2	56.8		0.33233(1)	···	0.42010(4)
$W_{0.8}Ir_2B_{7.2}$	B	B	0.5	0.2	99.3	1264	···	···	···
1100	Ir_4B_5	Ir_4B_5	0.0	43.3	56.7		1.0535(4)	0.2904(1) β = 91.15(3)	0.6103(1)
	τ_1	ReB_2	19.8	13.6	66.6 [a]		0.29266(2)	···	0.7538(1)
$W_{1.6}Ir_{0.8}B_{7.6}$	B	B	0.5	0.0	99.5	···	···	···	···
1100	τ_1	ReB_2	20.7	12.7	66.6[a]		0.29272(2)	···	0.7535(1)
	WB_2	WB_2	32.8	0.0	67.2		0.29855(2)	···	1.3887(4)
$WNi_{0.5}B_{8.5}$	B	B	0.3	1.4	98.3	1041	···	···	···
900	$W_{1-x}B_3$	$Mo_{1-x}B_3$	25.1	0.3	74.6		0.51979(5)	···	0.63366(7)
	NiB	TlI	0.1	50.6	49.3		···	···	···
$W_{0.6}Pd_{1.4}B_8$	B	B	0.4	0.1	99.5	963	···	···	···
900	$W_{1-x}B_3$	$Mo_{1-x}B_3$	21.8	0.1	78.1		0.51962(6)	···	0.6331(1)
	Pd_2B	$CaCl_2$	0.0	65.9	33.9		0.4691(1)	0.5135(2)	0.3136(2)
$W_{0.6}Pt_{1.4}B_8$	B	B	0.4	0.0	99.6	777	···	···	···
800	$W_{1-x}B_3$	$Mo_{1-x}B_3$	24.8	0.0	75.2		0.52006(2)	···	0.6333(2)
	$PtB_{0.67}$	$PtB_{0.67}$	0.3	59.1	40.6		0.3372(1)	0.5820(1)	0.4031(1)

[a] EPMA result normalized to 66.6 at.% B; $\tau_1 - W_{1-x}Ir_xB_2$

Table 6 Results from EPMA measurements and x-ray phase analysis for the alloys $W_{18}Ru_{13}B_{69}$, $W_{15}Os_{16}B_{69}$, $W_{18}Ir_{13}B_{69}$ and $V_{17}Ir_{16}B_{67}$ in as cast state and/or after annealing at 1500 °C

Sample	Phases	Structure type	Composition EPMA, at.%			Lattice parameter, nm		
			W,V	TM	B	*a*	*b*	*c*
$W_{13}Ru_{18}B_{69}$	B	B	···	0.4	99.6	···	···	···
as cast	WB_2	WB_2	30.6	1.7	67.7	0.29850(1)	···	1.3866(5)
	RuB_2	RuB_2	1.1	35.9	63.0	0.28715(3)	0.4641(1)	0.40494(5)
	$W_{1-x}Ru_xB_2$	ReB_2	12.3	21.1	66.6[a]	0.29027(1)	···	0.74673(2)
$W_{15}Os_{16}B_{69}$	B	B	0.1	0.9	99.0	···	···	···
1500	OsB_2	RuB_2	0.7	36.6	62.7	···	···	···
	$W_{1-x}Os_xB_2$	ReB_2	16.3	17.1	66.6[a]	0.29127(1)	···	0.7562(1)
$W_{18}Ir_{13}B_{69}$	B	B	0.4	···	99.6	···	···	···
as cast	WB_2	WB_2	32.3	0.1	67.6	0.29864(1)	···	1.3880(5)
	$W_{1-x}B_3$	$Mo_{1-x}B_3$	26.4	···	73.6	···	···	···
	Ir_4B_5	Ir_4B_5	···	42.8	57.2	···	···	···
	$W_{1-x}Ir_xB_2$	ReB_2	17.8	15.6	66.6[a]	0.29298(2)	···	0.7539(1)
$W_{18}Ir_{13}B_{69}$	B	B	0.1	0.1	99.8	···	···	···
1500	Ir_4B_5	Ir_4B_5	···	42.6	57.4	···	···	···
	$W_{1-x}Ir_xB_2$	ReB_2	19.2	14.2	66.6[a]	0.29263(1)	···	0.75404(8)
$V_{17}Ir_{16}B_{67}$	B	B	1.6	···	98.4	···	···	···
1500	VB_2	AlB_2	26.7	···	73.3	0.2999(1)	···	0.3056(1)
	Ir_4B_5	Ir_4B_5	···	44.2	55.8	1.0524(5)	0.29042(2) β = 91.12(4)	0.6102(1)

[a] EPMA results have been normalized to 66.6 at.% B

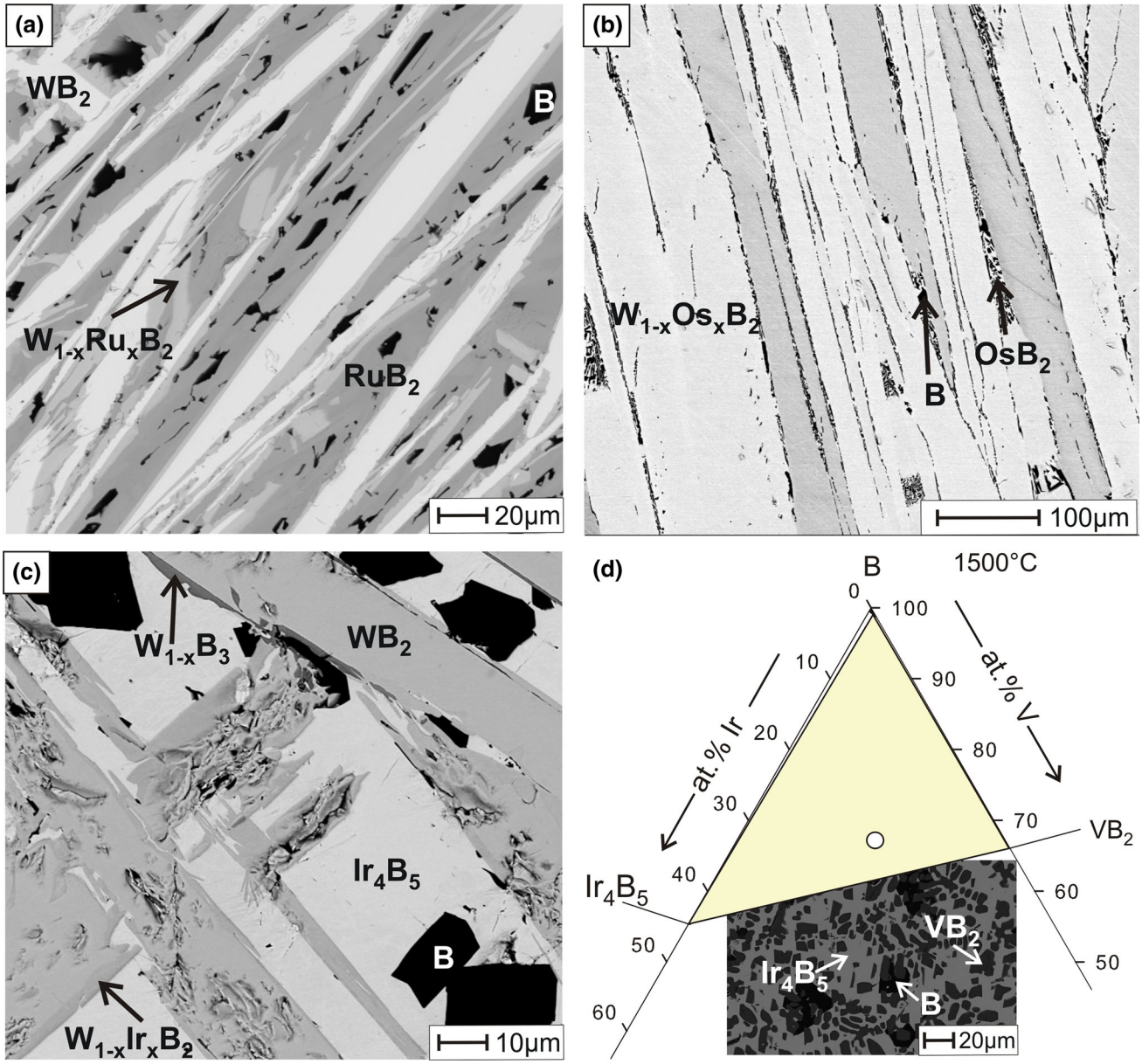

Fig. 5 SEM images of the alloys (a) $W_{13}Ru_{18}B_{69}$, (b) $W_{15}Os_{16}B_{69}$, (c) $W_{18}Ir_{13}B_{69}$ in as cast state and (d) partial isothermal section of the V-Ir-B phase diagram at 1500 °C

these results are not included in Fig. 4 and Table 6. On the other hand, annealing of the carefully mixed and cold pressed powders (W, Ru and B) at 900 to 1200 °C for 50 h in an argon atmosphere leads to homogeneous products.[12] Therefore we suggest that probably the diffusion at 1500 °C is to slow due to a rather high liquidus temperature. In case of the $W_{18}Ir_{13}B_{69}$ sample, annealing at 1500 °C leads to an almost single-phase sample $W_{0.6}Ir_{0.4}B_2$ with only about 2% impurity phases (Ir_4B_5 and B, see Table 6) but here even lower annealing temperatures (≥1100 °C) are sufficient. $W_{0.5}Os_{0.5}B_2$ forms congruently and the SEM image in Fig. 4b shows large grains and a three-phase eutectic at the grain boundaries consisting of $W_{0.5}Os_{0.5}B_2$, OsB_2 and B (see Table 6, results for the annealed alloy). The x-ray powder patterns of $W_{15}Os_{16}B_{69}$ in as cast state and after annealing contain sharp (h00, hk0) and rather diffuse and broad reflexions (00l, h0l). This has been observed already previously in some x-ray powder diffractograms of W-Ru-B[12] and Mo-Os-B[11] alloys and has been explained by irregular stacking faults in the crystal structure in the *c*-direction.[12] The possible formation of a ReB_2 isotypic compound has also been tested for V-Ir-B but neither in as cast state or after annealing at 1500 °C any ternary compound appeared. At 1500 °C, a three-phase equilibrium exists: B + VB_2 + Ir_4B_5 (see Fig. 5d and Table 6).

4. Conclusions

The reinvestigation of the crystal structure of $W_{1-x}B_3$ (≡ $WB_{\sim 4}$) by x-ray single crystal diffraction revealed isotypism with the $Mo_{1-x}B_3$ structure type (space group $P6_3/mmc$; a = 0.52012(1), c = 0.63315(3) nm; R_F=0.040). Boron occupies only the crystallographic site 12i (x,0,0) and tungsten the sites 2c (1/3,2/3,1/4) and 2b (0,0,1/4), the latter being filled to only about 72%. It should be emphasized that although $W_{1-x}B_3$ at about 80 at.% B is the metal boride richest in boron, it shows no directly linked three-dimensional boron framework. No solubility of Rh, Ir, Ni, Pd and Pt in $W_{1-x}B_3$ as well as of Rh in $Mo_{1-x}B_3$ has been found in as cast state and after annealing by EPMA measurements and by comparing the lattice parameter with those of the binary alloys. Furthermore, the boron rich parts of the corresponding isothermal sections W-TM-B (TM = Rh, Ir at 1100 °C, TM = Ni, Pd at 900 °C and TM = Pt at 800 °C) and Mo-Rh-B (at 1100 °C) have been established. Except for the W-Ir-B system, a three-phase equilibrium exists between β-boron, $W_{1-x}B_3$ or $Mo_{1-x}B_3$ and the transition metal boride richest in boron (RhB, NiB, Pd_2B, $PtB_{0,67}$). In the W-Ir-B system, two three-phase euilibria exist in the investigated part. βB is in equilibrium with Ir_4B_5 and τ_1-$W_{1-x}Ir_xB_2$ (ReB_2 type) and with WB_2 and τ_1. Formation and crystal structure of diborides $W_{1-x}TM_xB_2$ (TM = Ru, Os, Ir) with ReB_2 structure type (space group $P6_3/mmc$; a = 0.2900, c = 0.7475 nm) were studied by XPD and EPMA in as cast state and after annealing at 1500 °C. $W_{0.5}Os_{0.5}B_2$ (a = 0.29127(1), c = 0.7562(1) nm) forms directly from the melt, whereas $W_{0.4}Ru_{0.6}B_2$ (a = 0.29027(1), c = 0.74673 (2) nm) and $W_{0.6}Ir_{0.4}B_2$ (a = 0.29263(1), c = 0.75404(8) nm) are incongruently melting. Annealing at 1500 °C leads in case of the iridium compound to an almost single-phase product but the same procedure does not increase the amount of the ruthenium diboride.

Acknowledgment

This work was supported by the Austrian Science Fund FWF under Grant P22295. All EPMA measurements were carried out in the Faculty Centre for Nanostructure Research at the University of Vienna. Especially, we want to thank Dr. Puchegger for his help with the scanning electron microscope.

References

1. R. Riedel, Novel Ultrahard Materials, *Adv. Mater.*, 1994, **6**(7-8), p 549-560
2. S. Veprek, The Search for Novel Ultrahard Materials, *J. Vac. Sci. Technol. A*, 1999, **17**(5), p 2401-2420
3. J. Haines, J.M. Leger, and G. Bocquillon, Synthesis and Design of Superhard Materials, *Annu. Rev. Mater. Res.*, 2001, **31**, p 1-23
4. A.L. Ivanovskii, The Search for Novel Superhard and Incompressible Materials on the Basis of Higher Borides of *s*, *p*, *d* Metals, *J. Superhard Mater.*, 2011, **33**(2), p 73-87
5. V.V. Brazhkin, A.G. Lyapin, and R.J. Hemley, Harder Than Diamond: Dreams and Reality, *Phil. Mag.*, 2002, **82**, p 231-253
6. Q. Gu, G. Krauss, and W. Steurer, Transition Metal Borides: Superhard Versus Ultra Incompressible, *Adv. Mater.*, 2008, **20**, p 3620-3626
7. J.J. Gilman, R.W. Cumberland, and R.B. Kaner, Design of Hard Crystals, *Int. J. Refract. Metals Hard Mater.*, 2006, **24**(1-2), p 1-5
8. R. Mohammadi, A.T. Lech, M. Xie, B.E. Weaver, M.T. Yeung, S.H. Tolbert, and R.B. Kaner, Tungsten Tetraboride, An Inexpensive Superhard Material, *PNAS*, 2011, **108**(27), p 10958-10962
9. H.Y. Chung, J.M. Yang, M.B. Weinberger, S.H. Tolbert, J.B. Levine, R.B. Kaner, and A. Kavner, Synthesis of Ultra-Incompressible Superhard Rhenium Diboride at Ambient Pressure, *Science*, 2007, **316**(5823), p 436-439
10. J.B. Levine, S.L. Nguyen, S.E. Brown, H.I. Rasool, R.B. Kaner, and J.A. Wright, Preparation and Properties of Metallic, Superhard Rhenium Diboride Crystals, *J. Am. Chem. Soc.*, 2008, **130**, p 16953-16958
11. P. Rogl, H. Nowotny, and F. Benesovsky, Ternäre Komplexboride in den Dreistoffen: {Mo, W}-{Ru, Os}-B und W-Ir-B, Ternary Complex Borides in the Systems: {Mo, W}-{Ru, Os}-B and W-Ir-B, *Monatsh. Chem.*, 1970, **101**, p 850-854, in German
12. P. Rogl, H. Nowotny, and F. Benesovsky, Komplexboride mit ReB_2 Struktur, Complex borides with ReB_2 structure, Monatsh. Chem., 1970, **101**, 27-31, in German
13. V. Brazhkin, N. Dubrovinskaia, M. Nicol, N. Novikov, R. Riedel, V. Solozhenko, and Y. Zhao, What Does 'Harder Than Diamond' Mean?, *Nat. Mater.*, 2004, **3**, p 576-577
14. N. Dubrovinskaia, L. Dubrovinsky, and V.L. Solozhenko, Comment on 'Synthesis of Ultra-Incompressible Superhard Rhenium Diboride at Ambient Pressure', *Science*, 2007, **318**, p 1550c
15. A. Chretien and J. Helgorsky, Sur les borures de molybdene et de tungstene MoB_4 et WB_4 composes nouveaux, *Compt. Rend. Hebd. Seances Acad. Sci. Colon. (Paris)*, 1961, **252**(5), p 742-744, in French
16. E. Rudy, F. Benesovsky, and L. Toth, The Investigation of the Ternary Systems of the Group V and VI, Metals with Boron and Carbon, *Z. Metallkd.*, 1963, **54**, p 345-353, in German
17. P.A. Romans and M.P. Krug, Composition and Crystallographic Data for the Highest Boride of Tungsten, *Acta Crystallogr.*, 1966, **20**, p 313-315
18. H. Nowotny, H. Haschke, and F. Benesovsky, Bor-reiche Wolframboride, Boron Rich Tungsten Borides, *Monatsh. Chem.*, 1967, **98**, p 547-554, in German
19. T. Lundström and I. Rosenberg, The Crystal Structure of the Molybdenum Boride $Mo_{1-x}B_3$, *J. Solid State Chem.*, 1973, **6**, p 299-305
20. Y. Liang, X. Yuan, and W. Zhang, Thermodynamic Identification of Tungsten Borides, *Phys. Rev. B*, 2001, **83**, p 220102(R)
21. H. Gou, Z. Li, L.M. Wang, J. Lian, and Y. Wang, Peculiar Structure and Tensile Strength of WB_4: Nonstoichiometric Origin, *AIP Adv.*, 2012, **2**, p 012171
22. Y. Liang, Z. Fu, X. Yuan, S. Wang, Z. Zhong, and W. Zhang, An unexpected softening from WB_3 to WB_4, EPL, 2012, **98**(6), 66004
23. R.F. Zhang, D. Legut, Z.J. Lin, Y.S. Zhao, H.K. Mao, and S. Veprek, Stability and Strength of Transition-Metal Tetraborides and Triborides, *PRL*, 2012, **108**, p 255502
24. C. Zang, H. Sun, and C. Chen, Unexpectedly Low Indentation Strength of WB_3 and MoB_3 from First Principles, *Phys. Rev. B*, 2012, **86**, p 180101(R)
25. Q. Li, D. Zhou, W. Zheng, and Y. Ma, Global Structural Optimization of Tungsten Borides, *PRL*, 2013, **110**, p 136403

26. Y. Liang, X. Yuan, Z. Fu, Y. Li, and Z. Zhong, An Unusual Variation of Stability and Hardness in Molybdenum Borides, *Appl. Phys. Lett.*, 2012, **101**, p 181908
27. H. Haschke, Structural Chemical Investigations on Complex Borides and Carbides, as Well as on Silicides and Germanides of Rare Earth Metals PhD-Thesis, 1966, University of Vienna, in German
28. J.W. Simonson, D. Wu, S.J. Poon, and S.A. Wolf, Superconductivity in Transition Metal Doped MoB_4, *J. Supercond. Nov. Magn.*, 2010, **23**, p 417-422
29. N. Melnychenko-Koblyuk, A. Grytsiv, S. Berger, H. Kaldarar, H. Michor, F. Rohrbacher, E. Royanian, P. Rogl, H. Schmid, and G. Giester, Ternary Clathrates Ba-Cd-Ge: Phase Equilibria, Crystal Chemistry and Physical Properties, *J. Phys. Condens. Matter*, 2007, **19**, p 046203
30. G.M. Sheldrick, SHELX—Program, *Acta Cryst. A*, 2008, **64**, p 112-122
31. P. McArdle, K. Gilligan, D. Cunningham, R. Dark, and M. Mahon, Oscail—Program, *Cryst. Eng. Commun.*, 2004, **6**, p 303-309
32. J. Rodriguez-Carvajal, Recent Advances in Magnetic Structure Determination by Neutron Diffraction, *Physica B*, 1993, **192**, p 55-69
33. W.B. Pearson (1972), The Crystal Chemistry and Physics of Metals and Alloys, New York, USA: Wiley-Interscience, The 12-coordinated metallic radii in Table 4-4 of this book have been taken from: E. Teatum, K. Gschneidner, and J. Waber, Report LA-2345, US Department of Commerce, Washington, D.C., USA, 1960
34. X.-Q. Chen, C.L. Fu, M. Krcmar, and G.S. Painter, Electronic and Structural Origin of Ultraincompressibility of 5d Transition Metal Diborides MB_2 (M = W, Re, Os), *Phys. Rev. Lett.*, 2008, **100**, p 196403
35. P. Rogl, H. Nowotny, and F. Benesovsky, Über einige Komplexboride mit Platinmetallen, Complex Borides with Platinum Metals, *Monatsh. Chem.*, 1972, **103**, p 965-989, in German
36. H. Duschanek and P. Rogl, Critical Assessment and Thermodynamic Calculation of the Binary System Boron-Tungsten, *JPE*, 1995, **16**(2), p 150-161
37. E. Rudy and W. Windisch, *The Systems Mo-B and W-B, AFML-TR-2, Part I, Vol. III*, Wright Patterson Air Force Base, OH, USA, 1965, p 1-72
38. T.B. Massalski, *Binary Alloys Phase Diagrams*, 2nd ed., ASM International, Materials Park, Ohio, USA, 1990
39. P. Rogl, Phase Diagrams of Ternary Metal-Boron-Carbon Systems, Ed. Günter Effenberg; ASM International, Materials Park, Ohio 44043 (1988) p 1-566
40. A.J. Crespo, L.-E. Tergenius, and T. Lundström, The Solid Solution of 4d, 5d and SOMe p-Elements in ß-Rhombohedral Boron, *J. Less Common Met.*, 1981, **77**, p 147-150
41. M.F. Gabouskas, J.S. Kasper, and G.A. Slack, The Incorporation of Vanadium in ß-Rhombohedral Boron as Determined by Single-Crystal Diffractometry, *J. Solid State Chem.*, 1986, **63**, p 424-430
42. I. Smid and P. Rogl, "Phase Equilibria and Structural Chemistry in Ternary Systems: Transition Metal-Boron-Nitrogen", In Science of Hard Materials, Inst. Phys. Conf. Ser. No. 75. Chapter 4, Adam Hilger Ltd., 1986, p 249-257
43. B. Aronsson, E. Stenberg, and J. Åselius, Borides of Rhenium and the Platinum Metals. The Crystal Structure of Re_7B_3, ReB_3, Rh_7B_3, $RhB_{1.1}$ (approximate composition), $IrB_{1.1}$ (approximate composition) and PtB, *Acta Chem. Scand.*, 1960, **14**, p 733-741
44. J.B. Levine, S.H. Tolbert, and R.B. Kaner, Advances in the Search for Superhard Ultra-Incompressible Metal Borides, *Adv. Funct. Mater*, 2009, **19**, p 3519-3533
45. P. Rogl and E. Rudy, New Complex Borides with ReB_2- and Mo_2IrB_2-Type Structure, *J. Solid State Chem.*, 1978, **24**(2), p 175-181
46. T. Lundström, The Structure of Ru_2B_3 and $WB_{2.0}$ as Determined by Single Crystal Diffractometry, and Some Notes on the W-B System, *Arkiv Kemi*, 1969, **30**, p 115-127
47. R.B. Roof, Jr, and C.P. Kempter, New Orthorhombic Phase in the Ru-B and Os-B Systems, *J. Chem. Phys.*, 1962, **37**, p 1473-1476
48. B. Aronsson, The Crystal Structure of RuB_2, OsB_2 and $IrB_{1.35}$ and Some General Comments on the Crystal Chemistry of Borides in the Composition Range MeB-MeB_3, *Acta Chem. Scand.*, 1963, **17**, p 2036-2050
49. J.T. Norton, H. Blumenthal, and S.J. Sindeband, Structure of Diborides of Titanium, Zirconium, Columbium, Tantalum and Vanadium, *Trans. Am. Inst. Min. Metall. Pet. Eng.*, 1949, **185**, p 749-751
50. H.P. Klesnar, T.L. Aselage, B. Morosin, G.H. Kwei, and A.C. Lawson, The Diboride Compounds of Molybdenum: MoB_{2-x} and Mo_2B_{5-y}, *J. Alloys Compd.*, 1996, **241**, p 180-186